

## Supplemental Material

### Imaging viscoelastic properties of live cells by AFM: Power-law rheology on the nanoscale

F. M. Hecht,<sup>a†</sup> J. Rheinlaender,<sup>a†</sup> N. Schierbaum,<sup>a</sup> W. H. Goldmann,<sup>b</sup> B. Fabry,<sup>b</sup> and T. E. Schäffer<sup>\*a</sup>

<sup>a</sup> Institute of Applied Physics, University of Tübingen, Auf der Morgenstelle 10, 72076 Tübingen, Germany.

<sup>b</sup> Department of Physics, University of Erlangen-Nuremberg, Henkestraße 91, 91052 Erlangen, Germany.

† Both authors contributed equally to this publication.

\* E-mail: tilman.schaeffer@uni-tuebingen.de

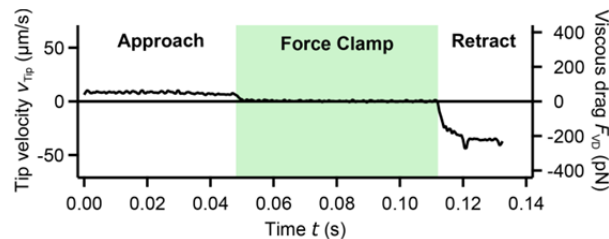


**Fig. S1** Estimation of the viscous drag force acting on the cantilever, generated by the cantilever's motion through the surrounding liquid, for the data shown in Figure 1. The tip velocity  $v_{\text{Tip}}(t)$  was calculated as the time derivative of the tip position,  $z(t) - d(t)$ . The viscous drag force  $F_{\text{VD}}$  was estimated from the tip velocity using  $F_{\text{VD}} = \mu v_{\text{Tip}}$ , where  $\mu$  is the viscous drag coefficient of the cantilever. For the cantilevers used here, the drag coefficient was determined as  $\mu = 6.2 \text{ pN} (\mu\text{m/s})^{-1}$  in a separate measurement (data not shown). We found that for the conditions used here, the influence of the tip-sample distance on the drag coefficient was negligible.

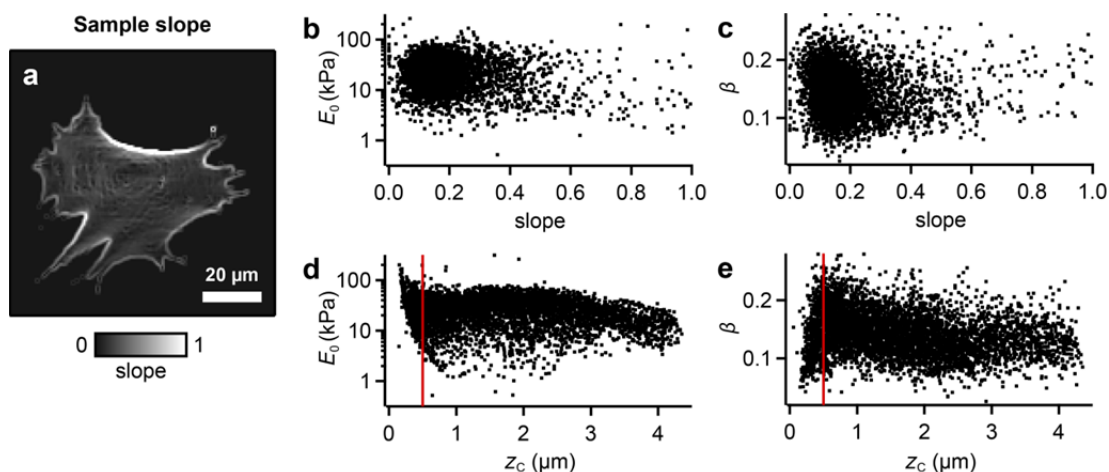


**Fig. S2** Correlation of modulus scaling parameter  $E_0$  and power-law exponent  $\beta$  vs sample slope and height for the cell shown in Figure 2. (a) Image of the sample slope,  $[(dz_c/dx)^2 + (dz_c/dy)^2]^{1/2}$ . (b)  $E_0$  and (c)  $\beta$  as a function of sample slope. Neither the modulus scaling parameter  $E_0$  nor the power-law exponent  $\beta$  show a significant correlation with sample slope. (d)  $E_0$  and (e)  $\beta$  as a function of sample height.  $E_0$  and  $\beta$  show a visible correlation only for heights smaller than about 500 nm (red line).

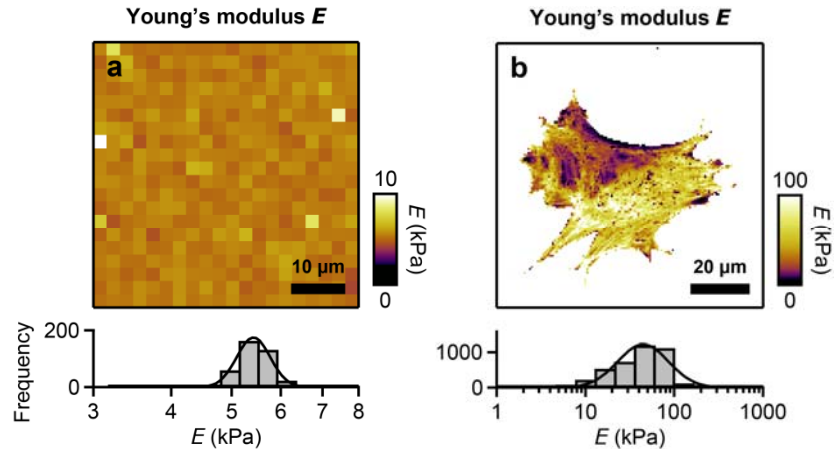


**Fig. S3** Maps of the apparent Young's modulus  $E$  of (a) the polyacrylamide (PAA) gel from Figure 2 and (b) the MEF vin-/ cell from Figure 3, obtained when applying a purely elastic contact model to the approach part of the force-distance curves. The Young's moduli are slightly larger than the respective modulus scaling parameters (Figure 2 and Figure 3, respectively).

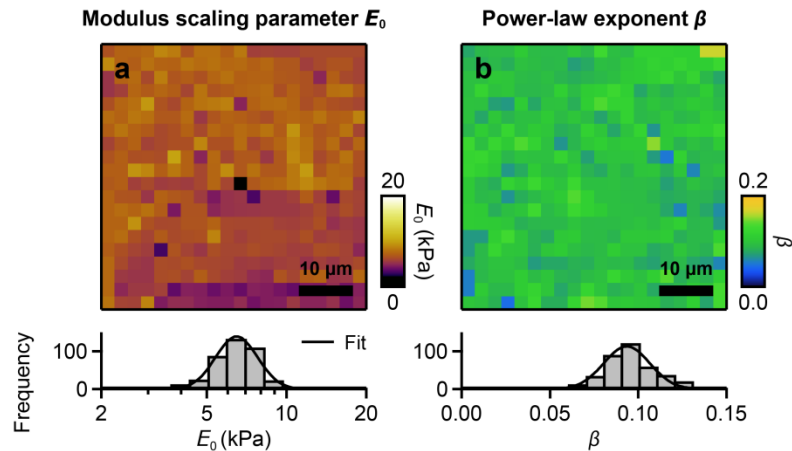


**Fig. S4** Force clamp force mapping (FCFM) on the same polyacrylamide (PAA) gel as in Figure 2, but recorded with a DNP type cantilever. (a) Map and histogram of the modulus scaling parameter  $E_0$ . (b) Map and histogram of the power-law exponent  $\beta$ . Pixel resolution is  $20 \times 20$  pixels. The mean values ( $E_0 = 6.4$  kPa and  $\beta = 0.092$ ) are in well agreement with the values obtained with the MLCT type cantilever from Figure 2 ( $E_0 = 5.3$  kPa and  $\beta = 0.091$ ), demonstrating the reliability of the FCFM method. The small difference in  $E_0$  could be explained by the inaccuracy in the determination of the cantilevers' spring constants (typically 10 – 20%).<sup>1</sup>

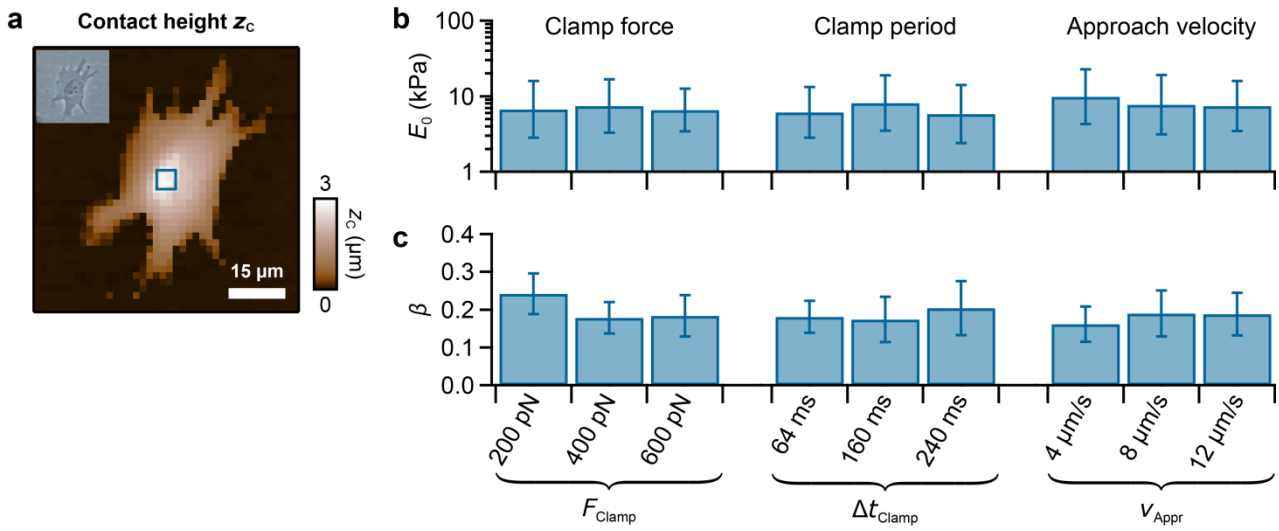


**Fig. S5** Power-law parameters  $E_0$  and  $\beta$  for different experimental parameters. (a) Map of contact height  $z_c$  of a MEF WT cell. (b) Modulus scaling parameter  $E_0$  and (c) power-law exponent  $\beta$  for different experimental parameters  $F_{\text{Clamp}}$ ,  $\Delta t_{\text{Clamp}}$ , and  $v_{\text{Appr}}$ , recorded within a small region on the cell (5  $\mu$ m  $\times$  5  $\mu$ m, 10  $\times$  10 pixels, marked by the box in panel a). Median  $\pm$  standard deviation is shown. Neither the mean values nor the standard deviations depend considerably on the different experimental parameters.

## References

- 1 C. T. Gibson, D. J. Johnson, C. Anderson, C. Abell and T. Rayment, *Rev. Sci. Instrum.*, 2004, 75, 565-567.